Journal Pre-proof

Extrusion 3D printing of nutraceutical oral dosage forms formulated with monoglycerides oleogels and phytosterols mixtures

Ivana M. Cotabarren, Sofia Cruces, Camila A. Palla

PII: S0963-9969(19)30562-9

DOI: https://doi.org/10.1016/j.foodres.2019.108676

Reference: FRIN 108676

To appear in: *Food Research International*

Received date: 26 July 2019

Revised date: 9 September 2019

Accepted date: 12 September 2019

Please cite this article as: I.M. Cotabarren, S. Cruces and C.A. Palla, Extrusion 3D printing of nutraceutical oral dosage forms formulated with monoglycerides oleogels and phytosterols mixtures, *Food Research International* (2019), https://doi.org/10.1016/j.foodres.2019.108676

Extrusion 3D printing of nutraceutical oral dosage forms formulated with monoglycerides oleogels and phytosterols mixtures

Ivana M. Cotabarren[a,b], Sofia Cruces[a], Camila A. Palla[a,b]

[a]Departamento de Ingeniería Química (DIQ) - Universidad Nacional del Sur (UNS)

[b]Planta Piloto de Ingeniería Química (PLAPIQUI, UNS-CONICET)

Bahía Blanca, Buenos Aires, Argentina

Abstract

Among the potential applications of 3D printing, the development of products with personalized characteristics in the area of food and nutraceuticals represents an important field that must still be explored. The aim of this work was to evaluate the production of nutraceutical oral forms by extrusion-based 3D printing (E3DP) using mixtures of monoglycerides (MG) oleogels and phytosterols (PS) as printing materials. These materials were obtained using MG (10 or 20 %wt), high oleic sunflower oil and variable amounts of PS (20 - 50 %wt PS/oleogel). An ad-hoc extrusion 3D printer composed of a heated syringe and a cooling build platform was used. Rheological tests were carried out to determine the mixtures gel point, in order to select appropriate printing temperatures, as well as the yield stress of the final materials. Hardness of printed forms was obtained by compression tests. Additionally, oral forms were produced by manual extrusion using molds for comparison. It was found that oral forms were successfully printed when using mixtures containing a maximum of 30 and 40 %wt PS/oleogel for oleogels formulated with 10 and 20 %wt of MG, respectively. Moreover, the best printed forms corresponded to the mixtures with the lowest gelation temperatures. These printed forms were structurally stable, with uniform weight and shape, and maximum hardness of 12.55 N. Hardness values of printed oral forms did not show a correlation with those obtained by manual extrusion using molds, indicating that this parameter was affected by solid composition, cooling rate and the fragility generated for layers superposition. In conclusion, it was demonstrated that mixtures of MG

oleogels and PS can be used for E3DP production of nutraceutical oral forms suggesting that oleogels have excellent potential as materials able to incorporate liposoluble active ingredients to be used as extrusion printing materials.

Keywords: 3D printing, nutraceuticals, oleogels, phytosterols, rheological properties, printer parameters.

1. Introduction

The last years of research have provided evidence of the role of nutraceuticals in the treatment and prevention of diseases, generating an increase in the area of research involving the food, nutraceutical and pharmaceutical industries (Braithwaite et al., 2014). A nutraceutical can be defined as “a food or component of the food that provides health and medicinal benefits, including the prevention and treatment of diseases” (Biesalski, 2001). Nutraceuticals may range from isolated nutrients, dietary supplements, and diets, to genetically engineered “designer” food, herbal products, and process product. These products are typically marketed in the form of a capsule, pill, powder or gel containing one or more healthy components.

Additionally, within the concept of nutrition and personalized medicine, the demand arises for technological solutions that allow the "tailor-made" production of oral administration formulations. In this sense, 3D printing emerges as a group of technologies of growing interest capable of producing customized formulas that have the desired shape, dimension and microstructure. 3D printing allows obtaining three-dimensional objects by building successive layers of material under the control of computer software (Alhnan et al., 2016). Among the available additive manufacturing technologies, extrusion-based 3D printing (E3DP) is the most used technology for food printing because of the wider range of available food materials that can be extruded to form a product. This method fabricates a 3D model by extruding semi-fluid mixtures and depositing them onto a platform, layer by layer (Huang, 2018). On the other hand, fused filament fabrication (FFF), which consists on depositing a filament of a molten polymer in successive horizontal planes, has been more popular among the printing of pharmaceutical solid oral forms. Both types of printers have different configurations; one of the mostly used is the Cartesian one (Fig. 1) due to its simplicity for maintenance and calibration.

Literature regarding nutraceuticals 3D printing is scarce. In fact, to the best of our knowledge, the only contribution on this field has been the study of Melocchi et al. (2018) that developed a 3D-printing nutraceutical delivery platform by FFF printing of capsular devices for the administration of dietary supplements. Regarding food 3D printing, different studies have explored the use of E3DP to generation of decorative shapes, fabrication of attractive food presentations, development of customized nutritional content, and exploration of new textures and flavors (Godoi, Prakash, & Bhandari, 2016; Hamilton, Alici, & in het Panhuis, 2018; Severini & Derossi, 2016). Regarding printing of pharmaceutical forms, some contributions using extrusion printing can be found for the production of bilayer tablets using immediate-release and sustained-release gels (Khaled et al., 2014), tablets with compartments having different actives with distinct releasing patterns (Khaled, Burley, Alexander, Yang, & Roberts, 2015), tablets with different geometries (Khaled et al., 2018), and for the fabrication of gastro-floating tablets (Li et al., 2017).

During the E3DP process, rheological properties of materials are critical for providing proper extrudability, binding of different layers together and supporting the weight of deposited layers (Liu, Zhang, Bhandari, & Yang, 2018). Although it is difficult for a soft material to meet all these requirements, materials that present changes in their physical properties by changes of temperature, e.g. from liquid to strong gel, can be more suitable for use as printable materials. Especially, saturated MG have shown promising ability to form elastic gels in liquid oil through oleogelation process. In order to prepare an oleogel, MG are melted in hot oil and by cooling of the mixture, the nucleation and growth of MG crystals take place producing a 3D-network that entraps oil (Palla, Giacomozzi, Genovese, & Carrin, 2017). Of particular concern is the fact that the physicochemical properties of MG oleogels are greatly affected by the MG crystallization behavior, which can be modified by the type of oil, cooling and shear rate, and by the addition of another component into the formulation. As consequence, oleogels present excellent potential to be used as printable material in the E3DP due to their physicochemical properties capable of being tailored as desired. Moreover, according to their hydrophobic nature, oleogels can dissolve high amounts of lipid-soluble bioactive molecules, allowing their release through different physiological pathways (Davidovich-Pinhas, 2016). Among the lipid-soluble bioactive molecules, phytosterols are of special interest in the treatment of

hypercholesterolemia and prevention of cardiovascular diseases. These natural compounds have structure and functionality similar to that of cholesterol, interfering in the intestinal absorption and allowing its excretion (Di Battista, Constenla, Ramírez Rigo, & Piña, 2017; Moss, Williams, & Ramji, 2018). Likewise, phytosterols in combination with monoglycerides have been used to obtain food-grade oleogels as alternative product to saturated fats or delivery agent of functional ingredients (Kouzounis, Lazaridou, & Katsanidis, 2017; Matheson, Dalkas, Clegg, & Euston, 2018; B. Sintang, Rimaux, Walle, Dewettinck, & Patel, 2016). Furthermore, the incorporation of phytosterols at certain ratios lead to the formation of semi-solid materials with a stronger oleogel networks and with increased hardness and gel strength respect to gels containing only monoglycerides (Kouzounis et al., 2017; B. Sintang et al., 2016).

Therefore, the aim of this work was to evaluate the production of nutraceutical oral forms by E3DP using mixtures of monoglycerides (MG) oleogels and phytosterols (PS) as printing materials. Firstly, mixtures with different MG concentration and PS ratios were prepared and characterized by rheological tests and polarized light microscopy (PLM) to evaluate their microstructure. After that, the prepared mixtures were used to print the designed oral forms. Additionally, oral forms were produced by manual extrusion using molds. The hardness of the obtained oral forms by both methodologies was determined in order to compare results. Furthermore, mixtures properties were related to printing parameters in order to obtain a better understanding of the process. Thus, the main innovative aspect of this contribution involves the use of the E3DP recently developed technology with oleogels as material with tailored rheological properties that are able to incorporate liposoluble active ingredients for personalized nutrition.

2. Methodology

2.1. Materials

A commercial food grade mixture of monoglycerides, Myverol 18-08 NP (MG), was generously donated by Kerry (Ireland). MG was composed of monoglycerides >90 % purity grade and its corresponding melting point was 72.0 °C according to the supplier's specification sheet. The MG fatty acid composition obtained by GLC analysis as fatty acid methyl esters (FAME) was 90.65 %wt of

stearic acid, 6.43 %wt of palmitic acid, and 1.53 %wt of arachidic acid. Phytosterols powder (PS) consisted in a mixture of 34 - 50 %wt β-sitosterol, 17 - 30 %wt campesterol, 22 - 30 %wt stigmasterol, and about of 2 - 7 %wt of other vegetable sterols (Advasterol 90 F, Advanced Organic Materials, Argentina). The PS melting point obtained by DSC was in the range of 132.8-137.9 °C. Refined high oleic sunflower oil (HOSO) (Cooperativa, Argentina) was purchased from a local grocery store.

2.2. Preparation of printing materials using oleogels and PS

Oleogels were formulated using 10 %wt or 20 %wt of MG in HOSO. Printing materials were formulated adding variable amounts of PS to oleogels, between 20 and 50 %wt PS/oleogel in order to obtain mixtures with high PS content (see Table 1). It is important to mention that the daily intake of PS is in the range of 150 - 400 mg, but a dose of 1.5 - 2 g is recommended for a cholesterol-lowering purpose (Cabral & Klein, 2017; Normén, Frohlich, & Trautwein, 2004). Firstly, HOSO was placed in a glass container system with a temperature-controlled water bath at temperatures between 80 - 95 °C under magnetic agitation at 300 rpm. After a period of 15 min, the correspondent amount of MG was poured to the container system followed by the addition of PS 10 min later. The mixture was kept under these conditions during 40 min. After that, molten samples were transferred to: i) the 3D printer syringe to be used as printing material or ii) syringes of similar characteristics to the one composing the 3D printer in order to evaluate the capacity of mixtures to flow through the nozzle, as it will be explained in section 2.6. Prior selecting the mentioned procedure for preparing the printing materials (addition of PS to molten mixture of MG and HOSO), it was assayed the mixture and homogenization of previously prepared oleogels (molten mixture of MG and HOSO cooled and stored at 5 °C during 48 h) with PS at 25 °C. However, the resulting materials led to very weak semi-solid forms when they were used for extrusion, therefore this methodology was discarded.

2.3. Rheological characterization

Rheological characterization of mixtures was conducted using a Paar Physica MCR 301 Rheometer (Anton Paar GmbH, Austria) equipped with a temperature control unit, a 50 mm plate-plate geometry, and a computerized data acquisition system (Rheoplus/32 V3.40). Oscillatory temperature sweep tests (strain 0.05 %, frequency 10 rad/s, and gap 0.8 mm) were carried out by cooling the molten samples from the specific preparation temperature to 20 °C applying a 2 °C/min rate. The gel point temperature (T_g) was determined as the crossover of the elastic (G') and viscous (G") modulus, i.e. where the loss tangent is equal to unity (Lupi et al., 2016). Subsequently, the following tests were performed at 20 °C: i) an oscillatory frequency sweep test (strain 0.05 %) from 10 to 100 rad/s; and strain sweep test at a fixed frequency (10 rad/s) with a strain range from 0.01 to 100 % to determine the critical yield strain (γ_c) as the onset value of the modulus curves. The product of critical strain and complex modulus (G^*) below γ_c was used to obtain the materials apparent yield stress (Y_s) since it correlates well with the yield stress determined from the viscosity maximum obtained in a stress ramp (TA Instruments, 2000, 2016). Temperature and frequency sweep measurements were performed in the linear viscoelastic region checked in a stress sweep, whereafter the strain was set at 0.05%. The tests were replicated at least three times for each sample.

2.4. Polarized light microscopy (PLM)

The microstructure of the printable materials formulated with mixtures of MG oleogels and variable amount of phytosterols obtained under same cooling conditions was visualized by PLM. For this purpose, a small droplet of the molten mixture was placed on a microscope slide and cover slip was then laid over the droplet to remove air. After that, gel was formed at 5 °C and kept at this temperature for 72 h (Palla et al., 2017). Digital optical micrographs were taken with an OLYMPUS BX51 optical microscope with polarized light (Olympus, Japan) using a 10x and 20x objective lens and digital DP50 camera. To obtain satisfactory reproducibility, four images were captured from each of the two replicates prepared.

2.5. 3D printing process

The E3DP is a digitally-controlled construction process that can build up complex 3D products layer by layer. It consists in loading the material inside the extrusion system, pushing the material out of the nozzle in a controlled manner, moving the material stream according to a predefined path, and bonding the deposited layer to form a coherent solid structure (J. Sun, Zhou, Yan, Huang, & Lin, 2016). In this work, an ad-hoc E3DP system adapted from a Prusa printer was used (Fig. 1). This system was designed to maintain the mixtures molten during the extrusion process and to immediately provide a cooling effect as they were deposited on the build platform that allows the mixtures to form gels. Thus, successive layers of semi-solid material were deposited to produce an object with the desired shape. Therefore, the E3DP system was built with the following three major parts: (i) an extrusion system, which consisted in a plastic syringe connected to a temperature-controlled heating device, interchangeable nozzles and a stepper motor system to displace the plunger, (ii) an X-Y-Z positioning system using stepper motors allowing the printer platform to move along the Y-axis and the printhead (extrusion system) to move in the X-Z axis, (iii) and a build platform refrigerated with a peltier cooler system with thermal grease between the peltier and the aluminum base to facilitate the heat transfer (temperature between 5 and 10 °C).

Three different nozzles were design in order to test their suitability for the evaluated printing materials (see Fig. 5 in section 3.3). All of them were metal nozzles in order to maintain the gels temperature during extrusion. Nozzle A presented an orifice of 0.83 mm with a flat cut respect to the surface, nozzle B had a conical tip that ended in a 0.40 mm orifice, while nozzle C was a needle type of tip with a transversal cut of 0.83 x 2.75 mm.

Prior to the printing process, a CAD file was generated to define the geometry of the nutraceutical oral solid form (OnShape, 2018). The design was performed following closely the dimensions of 1 g commercial pharmaceutical tablets (see CAD image in supplementary material). After that, the generated STL file was imported to the slicer software (Repetier, 2019) and several printing parameters were set (i.e., layer thickness, material infill, material flow, fan speed, printing speed, syringe temperature, build platform temperature, etc.).

The printing procedure used to obtain the solid forms consisted of the following steps:

1- The syringe was preheated to a temperature (T_S) higher than the mixture gel temperature (T_g) in order to maintain molted the printing material. With a manual sensor, the temperature along the heating system and the metal nozzle was registered.
2- The molten mixture was charged into the syringe by reverse action of the plunge motion motor, starting from the plunge in the lower position, in order to reduce the air volume to its minimum.
3- The build platform temperature (T_P) was allowed to stabilize by the peltier action.
4- The STL file was sent to the printer and the extrusion process begun.

It is important to mention that all printing tests were carried out using the same values of printing parameters and only a few were modified between samples when it was necessary to improve the printability of the mixtures.

2.6. Manual extrusion process

As previously mentioned, a manual extrusion process was carried out in order to evaluate the printability of the formulated mixtures and to produce oral dosage forms by gelling them in appropriate molds. In first place, a 10 mL syringe (2.10 mm diameter nozzle) was tempered before use by introducing and removing the hot mixture into the syringe several times. Subsequently, , the prepared mixture (Table 1) was pressed by hand through the syringe onto molds designed with the same shape of the oral dosage form, located on a platform of tempered glass at 5 °C. This step was quickly carried out to reduce heat loss from the mixture. After that, the samples were introduced into a refrigerator at 5 °C to complete the gelation process. At least six replicates were prepared for each type of mixture. After stored for 72 h at the aforementioned temperature, the molds were carefully removed and the samples hardness was determined via compression tests. The used molds were printed in ABS (Acrylonitrile Butadiene Styrene) using an available FFF printer (see molds CAD image in supplementary material).

2.7. Hardness

Hardness of solid form samples was determined by a texture profile analysis (TPA) of two-cycle compression test using a Texture Analyzer (TA Plus Lloyd Instruments, England) equipped with a 50 N load cell. After stored for 72 h at 5 °C, the samples were compressed in every cycle to 50 % of their original height using a cylindrical probe (25 mm diameter) at a crosshead speed of 1 mm/s. Afterwards, the probe was returned to the initial position at the same speed. Hardness was determined from the resulting force-time curve as the maximum force measured during the first compression cycle (Palla et al., 2017). The test was replicated at least four times for each type of samples.

2.8. Statistical Analysis

Statistical analysis was carried out by one-way ANOVA using OriginPro 9.1 software (OriginLab, USA). Fisher's post test was used for multiple comparisons between means with a significance level p-value ≤ 0.05. All the results were expressed as the mean ± standard deviation.

3. Results and discussion

3.1. Mixtures rheological characterization

Monitoring of the thermo-rheological behavior of the materials during processing is a key factor for the E3DP process (Torres, 2017). Based on this premise, the viscoelastic properties of evaluated mixtures as well as 10 %wt and 20 %wt MG oleogels were determined as a function of temperature (Fig. 2). The G' curves were characterized by different regions: i) a region of very low G' values at initial stages of cooling corresponding to the molten mixture; ii) a sudden increase in G' values corresponding to the gelation of samples, in which the crystalline network was being formed; and iii) a posterior increased of G', in which one or two slope changes in the G' curves were observed, until reaching the quasi-equilibrium value at 20 °C. The behavior showed by both MG oleogels when decreasing the temperature was in agreement with results previously reported for oleogels formulated with MG and different

vegetables oils (Lupi et al., 2016; Ojijo, Neeman, Eger, & Shimoni, 2004; Palla et al., 2017). Based on previously obtained DSC results, the slope change in the G' curve which occurred between 38 and 41 °C could be related to MG transition to a second crystal polymorph (Palla, de Vicente, Carrín, & Gálvez Ruiz, 2019). Oleogels containing PS showed an additional inflection on the G' curves around 50 - 55 °C, this change may be caused by growth of crystals in a perpendicular direction or by aggregation of the crystals in a lateral direction that reinforces the network (Kouzounis et al., 2017). The temperature at which the G'/G" crossover was observed was identified as the gelation point (T_g). This temperature was 59.05 and 64.97 °C for oleogels formulated with 10 and 20 %wt of MG, respectively. In general, with the addition of PS to oleogels the T_g was modified (Table 1). For mixtures composed by 10 %wt MG, an increase in PS content produced a rise of the T_g average value. For mixtures composed by 20 %wt MG, the addition of PS generated a decrease (M20-20), an increase (M20-40 and M20-50) or not changed the T_g oleogel value (M20-30). It is interesting to note that mixtures that presented an increment in T_g were formulated with a ratio equal or greater than 2 gPS/gMG. This suggests that beyond a certain amount of PS the gelation process was promoted. For ratios smaller than 1 gPS/gMG an inhibition of the gelation process was observed, as well as reported by Kouzounis et al. (2017).

From the oscillatory frequency sweep tests, it was found that all the mixtures showed a gel-like behavior with the predominance of G' over G" independent of the frequency, and the ratio G"/G' resulted lower than 0.06 (data not shown) which indicated that the evaluated mixtures were able to form strong gels (Patel, Babaahmadi, Lesaffer, & Dewettinck, 2015). The elastic modulus of the gels ranged around 4.1 x10^5 and 2.8 x10^6 Pa and 2.0 x10^6 and 2.7 x10^6 Pa for mixtures containing 10 and 20 %wt of MG, respectively, resulting higher than those corresponding to MG oleogels. As it can be seen from Fig. 2, G' increased with the increase in PS concentration for samples formulated with 10 %wt of MG in oleogels. However, the effect of rising the PS amount was not as marked in samples formulated with 20 %wt of MG in oleogels. The reinforcement of the gel network by incorporation of PS into monoglycerides in-oil dispersions has been reported by Bin Sintang et al. (2017) and Kouzounis et al. (2017). These authors suggested that the incorporation of PS into MG oleogels reduced the clustering of MG crystals, achieving a better spatial distribution of the crystalline network that

improves the viscoelastic properties. In the present work, where mixtures containing higher proportions of PS were evaluated, the increment in elasticity was correlated with the solid content in the printable materials, but also could be attributed to a certain point to a better MG crystals distribution.

Strain sweeps are a valuable tool for characterizing structured fluid systems. These measurements not only allow identifying fluids and soft solids as being linear or non-linear viscoelastic, but they also enable yield stresses to be calculated with good reproducibility. The apparent yield stress of fat materials can be used to correlate with spreadability and material stability (A. Sun & Gunasekaran, 2009). G' curves from strain sweep tests of evaluated gels showed different behavior (Fig. 2.e and 2.f). Firstly, G' was kept constant at low values of strain for all materials. After that, both MG oleogels as well as samples formulated with 20 and 30 %wt of PS showed that when increasing the strain above a critical strain value the material experimented structural breakdown. Although, a wider linear viscoelastic region for mixtures containing PS was observed (30 %wt > 20%wt > oleogel) which indicates a more compact gel network structure due to the PS incorporation. In the case of samples formulated with 40 and 50 %wt of PS, the test could not be completed. Due to the hardness of these materials, the strain values higher than 0.7 - 1 % were not able to be achieved for the equipment since maximum torque was reached. This made evident the high degree of structuration developed in these materials and their excellent stability. Related to the apparent yield stress, it was found a significant increase in mixtures containing 20 %wt of MG for same ratio of PS (Table 1). The incorporation of PS produced higher levels of stabilization and its effect was more noticeable in gels formulated with 10 %wt of MG. The yield stress values of gels in which this parameter could be determined, ranged between 1738 and 5275 Pa (only printable materials are considered). Previous works based on E3DP of food materials have reported yield stress values between 195 and 370 Pa for pastes formulated with mashed potatoes with addition of potato starch (Liu et al., 2018), 687 and 1095 Pa (at 20 °C) for two commercially available breakfast spreads, Vegemite and Marmite, respectively (Hamilton et al., 2018), and between 5.3 and 99.9 Pa for food pastes made of protein, starch, and fiber-rich materials (Lille, Nurmela, Nordlund, Metsä-Kortelainen, & Sozer, 2018). This comparison highlights not only the greater stability of the mixtures evaluated in this work, but also the versatility of

oleogels to be used as 3D printing material allowing to have first a fluid material that could be easily extruded by the syringe to later become into a strong semisolid during layer depositions. It is important to note that the printing food materials used in the previously cited works are pastes that present the same rheological properties during the extrusion as well as the deposition processes. Therefore, syringes need to exert high pressures in order to extrude the material through the nozzles.

3.2. Polarized light microscopy

Fig. 3 presents PLM microscopic images of the 10 %wt MG oleogel and of a mixture of PS in HOSO in order to identify contributions of individual components in the mixtures. MG crystals in oleogels appeared distributed in irregular, elongated, fibrillar or needle-like shapes, which was in agreement with observations reported in previous works (López-Martínez et al., 2014; Lupi et al., 2016). On the other hand, PS samples showed multiple morphologies with aggregates consisting of fibrous, spherulite, and plate-like crystals (B. Sintang et al., 2016). Micrographs of mixtures containing MG oleogels and an increasing amount of PS are shown in Fig. 4. Structures composed of small crystals and more uniformly distributed were obtained at the lowest ratios of PS, whereas aggregates of PS were clearly distinguishable at the highest ratios of PS. Kouzounis et al. (2017) reported that when larger quantities of phytosterols are added to the mixtures, excess phytosterols cannot fully interact with the monoglycerides and tend to crystallize on their own. Consistent with that finding, in this work this effect resulted attenuated in mixtures containing 20 %wt of MG.

3.3. 3D printing process

Previously to the printing tests listed in Table 2, the three types of nozzles were tested for M10-20 (Fig. 5). The best printing performance was obtained using nozzle A, therefore this was selected to be used for all the experimental work. Nozzle B presented a very small orifice that was easily blocked with the material that gelled. In fact, it can be seen in Fig. 5 that the solid form was half printed due to nozzle blockage. Regarding nozzle C, the tip was too sharp and the deposited material was broken as the printing process advanced.

The manual extrusion process showed that all the molten mixtures, even those that presented high PS content, were able to pass through a syringe. In fact, it was observed that PS was completely solubilized in the oleogel at the preparation temperatures. Therefore, a total of 8 mixtures were tested in the E3DP system. For all printing test, the values of layer thickness, first layer thickness, printing speed, shell thickness, infill pattern, and flow percentage remained constant, while the values of syringe temperature, infill percentage and fan speed were modified, when necessary, as shown in Table 2.

Layer thickness defines the height of each layer of deposited material. In this study, a first layer of 0.2 mm was chosen to allow material to form a thin layer for adherence of the solid form on the build platform, followed by 1 mm layers. On overall, all solid forms were printed with 7 layers of materials. It is important to note that the printing material leaves the nozzle as liquid but becomes gel when comes into contact with the built platform; therefore, the actual layer height depends on the individual gel properties, even if the nozzle moved exactly 1 mm on Z direction between layers. Printing speed is the nozzle displacement velocity, which was set equal for all printing tests. Shell thickness is the width of the outer perimeter printed in each layer; again the actual value for this parameter depends on material properties. The infill pattern refers to the movements described by the nozzle when printing the interior paths of each layer; since the nozzle tends to drag the previously extruded material, the best option for these solid forms was to set the pattern as concentric lines starting from the outer perimeters. Flow percentage refers to how much material is to be extruded during the printing; this variable was kept in the slicer software nominal value.

Regarding the parameters that where slightly modified during printing, the most important was the syringe temperature which was directly related to the mixtures gel temperature. As presented in the previous section, samples formulated with the highest PS content presented the highest T_g values, therefore required the highest T_s. In general, the syringe temperature was set at least 30 °C higher than the mixtures T_g values in order to compensate the system heating lost, allowing a nozzle tip temperature higher than T_g. Otherwise, the mixtures gelled in the syringe before reaching the build platform. Regarding the infill density, this parameter states how much material is to be printed in the inner lines of each layer; the higher the infill density is, the more lines the extruder will print in each layer.

Therefore, when the mixture PS content increased, it was necessary to reduce the amount of material extruded to allow a better form printability (Table 2). This was because those mixtures tended to gel faster, as consequence the printed lines were dragged by the nozzle, breaking the structure if too much material was extruded. Fan speed was mainly set to zero, except for the last layers of some mixtures where an extra cooling action was required in order to compensate the temperature gradient generated between the last deposited layer and the cooled build platform.

Fig. 6 and 7 illustrate the effect of the mixture composition and printing parameters on materials printability by showing three examples of solid forms printed in each case. It was found that the higher the PS content was, the more difficult the material to print. Since this material formed gel faster, it tended to block the nozzle or to be dragged by the nozzle tip. This can be observed by comparing solid forms from M10-20 to M10-40 and from M20-20 to M20-50 that clearly showed a geometry deformation as PS content increased. Even if these gels presented better stability according the rheology results, the final solid form was affected by the nozzle dragging effect. Furthermore, at higher MG content the shape of the printed solid form improved. This can be noted by comparing printed samples formulated with the same PS content: M10-20 with M20-20, M10-30 with M20-30, and M10-40 with M20-40. Probably, the decrease in gel temperature with MG content favored the building of the solid form since the mixtures remained partially liquid during the time each layer was printed. As it can be seen in Fig. 7, it was not possible to successfully print a complete oral dosage form using the mixture M20-50 due to the high PS content, at least under the tested printer settings. Regarding M10-50, although several printing attempts were conducted, it was not possible to print even a few layers of material.

Overall, it was observed that the best printed forms were obtained with M10-20, M20-20 and M20-30 mixtures. Therefore, the PS content corresponding to these oral forms ranged from 167 mg to 230 mg for unit dose. Moreover, 285 mg for unit dose can be obtained using the mixture M20-40.

3.4. Weight uniformity

All the produced solid forms were individually weighed after the printing process and prior to the texture analysis. The average weight for each mixture and its corresponding deviation is shown in Table 1. Even if there is no clear regulation regarding nutraceutical products, the European Pharmacopoeia (F. E., 2018) recommends for solid tablets that the deviation in weight percentage should be <5 %. As it can be seen from the measurements, printed solid forms were produced with a high degree of repeatability of weight, close to the recommended standards.

3.5. Oral forms texture analysis

The mechanical properties of formulations designed for oral administration are key to determine the product handling. In this study, the TPA test was used with the aim of characterizing the solid oral forms produced by both E3DP and manual extrusion using different parameters such as hardness, cohesiveness, and adhesiveness, which are obtained from the resultant force-time plot. However, it was observed that in most of the evaluated samples a portion of the material remained on the probe after the first compression cycle. Consequently, only data obtained from the first compression cycle could be properly analyzed being hardness the main determined parameter. Significant differences were found in the hardness values of printed oral forms formulated with the tested mixtures (Fig. 8). In general, the hardness increased with the increase of PS content for both 10 %wt MG and 20 %wt MG oleogels, except for M10-40. This result suggests that, at a constant amount of MG in oleogels, an increase of the solid content produced printable materials with firmer structure. However, this finding's applicability may be somewhat limited by the printing process since it was noted that the mixtures containing 50 %wt of PS were not able to produce the desired 3D design. Moreover, the mixture M10-40 showed a non-uniform deposition of layers that generated defected printed forms (Fig. 6) with a lower resistance than it could be expected based on its composition.

Of particular interest in this work was to evaluate the hardness values of printed oral forms in comparison with those obtained using manual extrusion into molds. It was hypothesized that the rapid cooling of the oleogel molten mixtures taking place during the

deposition of a fine layer of material on the cooled building platform could favor the MG crystallization process, allowing to obtain a material composed of small crystals with improved mechanical properties. Conversely, it was also expected that the oleogel molten mixture cooled into molds experiences a cooling temperature profile -a slower global cooling process- until it reaches the stabilization temperature (5 °C), which would lead to the formation of a material with a microstructure characterized by bigger crystals. This hypothesis could be partially confirmed since different results of hardness were obtained depending on the mixture composition. For mixtures composed by 10 %wt MG, hardness values of printed oral forms were lower, similar and higher than the ones obtained with oral forms produced by manual extrusion using M10-20, M10-30, and M10-40, respectively. For mixtures composed by 20 %wt MG, regardless of the amount of PS, it was found that the hardness values of printed oral forms were significantly lower than those obtained for oral forms produced by manual extrusion. This different behavior found in the printed samples suggests that the hardness was not only a function of solid composition and cooling rate but also of other factors such as interactions between crystals conforming the material and fragility generated for layers superposition. On the other hand, an important finding to emerge from these comparisons was that the average deviation of hardness mean values was 0.63 vs. 1.23 N for samples obtained using E3DP and manual extrusion into molds, respectively, which highlights the superiority of E3DP to produce oral forms with more uniform properties.

Related to the effect of mixture composition on hardness of the oral forms produced by manual extrusion into molds, it was found that samples prepared with 20 %wt MG oleogels showed in average an increase in hardness between 172 and 303 % compared to samples prepared with 10 %wt MG, for a same PS content. These results are in agreement with those obtained by Kouzounis et al. (2017), who studied mechanical properties of oleogels formulated with different MG:PS ratios (20 %wt of gelator) using a penetration test. These authors reported that samples prepared with 3:1 ratio were harder than those corresponding to 1:1 ratio. In that case, oleogels were formed by cooling the molten mixtures in containers, in a similar way to samples in molds but different to E3DP, which indicates that processing of mixtures, mainly cooling process, was also a determining factor on samples mechanical properties.

4. Conclusion

In this work, the production of nutraceutical oral forms by formulating different mixtures of monoglycerides oleogels and phytosterols was evaluated using an ad-hoc E3DP printer with a heated syringe and a cooling build platform. The effect of different MG and PS proportions on rheological properties and final quality of printed forms was investigated. It was observed that successfully printed forms were obtained when using mixtures containing a maximum of 30 and 40 %wt PS/oleogel for oleogels formulated with 10 and 20 %wt of MG, respectively. Moreover, the best printed forms corresponded to the mixtures with the lowest gelation temperatures. Probably, the decrease in gel temperature favored the building of the dosage forms since the mixtures remained partially liquid during the time each layer was printed. Consequently, the PS content in successfully printed oral forms ranged from 230 mg to 285 mg for unit dose. Hardness values of printed oral forms did not show a correlation with those obtained by manual extrusion using molds, indicating that this parameter was affected by solid composition, cooling rate and the fragility generated for layers superposition. Furthermore, the relatively high hardness values obtained for the printed forms showed products with potential good performance for their handling, dispensing, packaging, etc. Finally, the printed forms were produced with a high degree of weight repeatability, close to the recommended standards.

However, further work is needed to explore different printing settings to reach printed forms with more PS content per unit dose, as well as to evaluate liberation of the active ingredient through dissolution and digestion tests. In conclusion, it was demonstrated that mixtures of monoglycerides oleogels and phytosterols can be used for E3DP production of nutraceutical oral forms indicating that oleogels have excellent potential as materials able to incorporate liposoluble active ingredients to be used as extrusion printing materials.

Acknowledgment

The authors acknowledge the financial support by the Consejo Nacional de Investigaciones Científicas y Técnicas (PIP 1122015 - 0100156 CO), Agencia Nacional de Promoción Científica y Tecnológica (PICT 2017 - 1522) and the Universidad Nacional del Sur (PGI 24/M152) in Argentina. The authors also express their gratitude to Eng. Diego Colaneri for his technical assistance and to the companies Cooperativa Obrera Ltda. de Consumo y Vivienda and Kerry Inc., which kindly provided the phytosterols and monoglycerides, respectively.

Conflict of interest

The authors have no conflict of interest to declare.

References

Alhnan, M. A., Okwuosa, T. C., Sadia, M., Wan, K. W., Ahmed, W., & Arafat, B. (2016). Emergence of 3D Printed Dosage Forms: Opportunities and Challenges. *Pharmaceutical Research*, *33*(8), 1817–1832. https://doi.org/10.1007/s11095-016-1933-1

Biesalski, H. K. (2001). Nutraceuticals: the link between nutrition and medicine. In *Nutraceuticals in health and disease prevention*. USA: Marcel Deckker Inc.

Bin Sintang, M. D., Danthine, S., Brown, A., Van de Walle, D., Patel, A. R., Tavernier, I., … Dewettinck, K. (2017). Phytosterols-induced viscoelasticity of oleogels prepared by using monoglycerides. *Food Research International*, *100*(August), 832–840. https://doi.org/10.1016/j.foodres.2017.07.079

Braithwaite, M. C., Tyagi, C., Tomar, L. K., Kumar, P., Choonara, Y. E., & Pillay, V. (2014). Nutraceutical-based therapeutics and formulation strategies augmenting their efficiency to complement modern medicine: An overview. *J. Funct. Foods*, *6*, 82–99.

Cabral, C. E., & Klein, M. R. S. T. (2017). Phytosterols in the Treatment of Hypercholesterolemia and Prevention of Cardiovascular Diseases. *Arquivos Brasileiros de Cardiologia*, 475–482. https://doi.org/10.5935/abc.20170158

Davidovich-Pinhas, M. (2016). Oleogels: a promising tool for delivery of hydrophobic bioactive molecules. *Therapeutic Delivery*, *7*(1), 649–655.

Di Battista, C. A., Constenla, D., Ramírez Rigo, M. V., & Piña, J. (2017). Process analysis and global optimization for the microencapsulation of phytosterols by spray drying. *Powder Technology*, *321*, 55–65. https://doi.org/10.1016/j.powtec.2017.08.008

F. E. (2018). *European Pharmacopeia* (9th Editio). Retrieved from https://www.edqm.eu/en/european-pharmacopoeia-ph-eur-9th-edition.

Godoi, F. C., Prakash, S., & Bhandari, B. R. (2016). 3d printing technologies applied for food design: Status and prospects. *Journal of Food Engineering*, *179*, 44–54. https://doi.org/10.1016/j.jfoodeng.2016.01.025

Hamilton, C. A., Alici, G., & in het Panhuis, M. (2018). 3D printing Vegemite and Marmite: Redefining "breadboards." *Journal of Food Engineering*, *220*, 83–88. https://doi.org/10.1016/j.jfoodeng.2017.01.008

Huang, C. Y. (2018). Extrusion-based 3D Printing and Characterization of Edible Materials. Retrieved from https://uwspace.uwaterloo.ca/handle/10012/12899

Khaled, S. A., Alexander, M. R., Irvine, D. J., Wildman, R. D., Wallace, M. J., Sharpe, S., … Roberts, C. J. (2018). Extrusion 3D Printing of Paracetamol Tablets from a Single Formulation with Tunable Release Profiles Through Control of Tablet Geometry. *AAPS PharmSciTech*. https://doi.org/10.1208/s12249-018-1107-z

Khaled, S. A., Burley, J. C., Alexander, M. R., & Roberts, C. J. (2014). Desktop 3D printing of controlled release pharmaceutical bilayer tablets. *International Journal of Pharmaceutics*, *461*(1–2), 105–111. https://doi.org/10.1016/j.ijpharm.2013.11.021

Khaled, S. A., Burley, J. C., Alexander, M. R., Yang, J., & Roberts, C. J. (2015). 3D printing of tablets containing multiple drugs with defined release profiles. *International Journal of Pharmaceutics*, *494*(2), 643–650. https://doi.org/10.1016/j.ijpharm.2015.07.067

Kouzounis, D., Lazaridou, A., & Katsanidis, E. (2017). Partial replacement of animal fat by oleogels structured with monoglycerides

and phytosterols in frankfurter sausages. *Meat Science*, *130*(February), 38–46. https://doi.org/10.1016/j.meatsci.2017.04.004

Li, Q., Guan, X., Cui, M., Zhu, Z., Chen, K., Wen, H., … Pan, W. (2017). Preparation and investigation of novel gastro-floating tablets with 3D extrusion-based printing. *International Journal of Pharmaceutics*, *535*(1–2), 325–332. https://doi.org/10.1016/j.ijpharm.2017.10.037

Lille, M., Nurmela, A., Nordlund, E., Metsä-Kortelainen, S., & Sozer, N. (2018). Applicability of protein and fiber-rich food materials in extrusion-based 3D printing. *Journal of Food Engineering*, *220*, 20–27. https://doi.org/10.1016/j.jfoodeng.2017.04.034

Liu, Z., Zhang, M., Bhandari, B., & Yang, C. (2018). Impact of rheological properties of mashed potatoes on 3D printing. *Journal of Food Engineering*, *220*, 76–82. https://doi.org/10.1016/j.jfoodeng.2017.04.017

López-Martínez, A., Morales-Rueda, J. A., Dibildox-Alvarado, E., Charó-Alonso, M. A., Marangoni, A. G., & Toro-Vazquez, J. F. (2014). Comparing the crystallization and rheological behavior of organogels developed by pure and commercial monoglycerides in vegetable oil. *Food Research International*, *64*, 946–957. https://doi.org/10.1016/j.foodres.2014.08.029

Lupi, F. R., Greco, V., Baldino, N., de Cindio, B., Fischer, P., & Gabriele, D. (2016). The effects of intermolecular interactions on the physical properties of organogels in edible oils. *Journal of Colloid and Interface Science*, *483*, 154–164. https://doi.org/10.1016/j.jcis.2016.08.009

Matheson, A., Dalkas, G., Clegg, P. S., & Euston, S. R. (2018). Phytosterol-based edible oleogels: A novel way of replacing saturated fat in food. *Nutrition Bulletin*, *43*(2), 189–194. https://doi.org/10.1111/nbu.12325

Melocchi, A., Parietti, F., Maccagnan, S., Ortenzi, M. A., Antenucci, S., Briatico-vangosa, F., … Zema, L. (2018). Industrial Development of a 3D-Printed Nutraceutical Delivery Platform in the Form of a Multicompartment HPC Capsule. https://doi.org/10.1208/s12249-018-1029-9

Moss, J. W. E., Williams, J. O., & Ramji, D. P. (2018). Nutraceuticals as therapeutic agents for atherosclerosis. *Biochimica et Biophysica Acta - Molecular Basis of Disease*, *1864*(5), 1562–1572. https://doi.org/10.1016/j.bbadis.2018.02.006

Normén, L., Frohlich, J., & Trautwein, E. (2004). Role of plant sterols in cholesterol lowering. In P. C. Dutta (Ed.), *Phytosterols as Functional Food Components and Nutraceuticals* (pp. 243–315). New York, United States: Marcel Dekker Inc.

Ojijo, N. K. O., Neeman, I., Eger, S., & Shimoni, E. (2004). Effects of monoglyceride content, cooling rate and shear on the rheological properties of olive oil/monoglyceride gel networks. *Journal of the Science of Food and Agriculture*, *84*(12), 1585–1593. https://doi.org/10.1002/jsfa.1831

OnShape. (2018). OnShape. Retrieved from https://www.onshape.com/

Palla, C., de Vicente, J., Carrín, M. E., & Gálvez Ruiz, M. J. (2019). Effects of cooling temperature profiles on the monoglycerides oleogel properties: A rheo-microscopy study. *Food Research International Journal*, *125*. https://doi.org/10.1016/j.foodres.2019.108613

Palla, C., Giacomozzi, A., Genovese, D. B., & Carrin, M. E. (2017). Multi-objective optimization of high oleic sunflower oil and monoglycerides oleogels: Searching for rheological and textural properties similar to margarine. *Food Structure*, *12*, 1–14. https://doi.org/10.1016/j.foostr.2017.02.005

Patel, A. R., Babaahmadi, M., Lesaffer, A., & Dewettinck, K. (2015). Rheological Profiling of Organogels Prepared at Critical Gelling Concentrations of Natural Waxes in a Triacylglycerol Solvent. *Journal of Agricultural and Food Chemistry*, *63*(19), 4862–4869. https://doi.org/10.1021/acs.jafc.5b01548

Repetier. (2019). Hot-World GmbH & Co. KG. Retrieved from https://www.repetier.com/

Severini, C., & Derossi, A. (2016). Could the 3D Printing Technology be a Useful Strategy to Obtain Customized Nutrition? *Journal of Clinical Gastroenterology*, *50*(December), S175–S178. https://doi.org/10.1097/MCG.0000000000000705

Sintang, B., Rimaux, T., Walle, D. Van De, Dewettinck, K., & Patel, A. R. (2016). Studying the oil structuring properties of monoglycerides and phytosterols mixtures. *European Journal of Lipid Science and Technology A*.

Sun, A., & Gunasekaran, S. (2009). *Yield stress in foods: Measurements and applications*. *International Journal of Food Properties*

(Vol. 12). https://doi.org/10.1080/10942910802308502

Sun, J., Zhou, W., Yan, L., Huang, D., & Lin, L. ya. (2016). Extrusion-based food printing for digitalized food design and nutrition control. *Journal of Food Engineering*, 1–11. https://doi.org/10.1016/j.jfoodeng.2017.02.028

TA Instruments. (2000). Rheological Techniques for Yield Stress Analysis. Retrieved July 6, 2019, from http://www.tainstruments.com/pdf/literature/RH025.pdf

TA Instruments. (2016). Understanding rheology of structured fluids. Retrieved July 6, 2019, from http://www.tainstruments.com/pdf/literature/AAN016_V1_U_StructFluids.pdf

Torres, M. D. (2017). Role of the Rheology in the New Emerging Technologies as 3D Printing. *Rheology: Open Access*, *1*(2), 3–4.

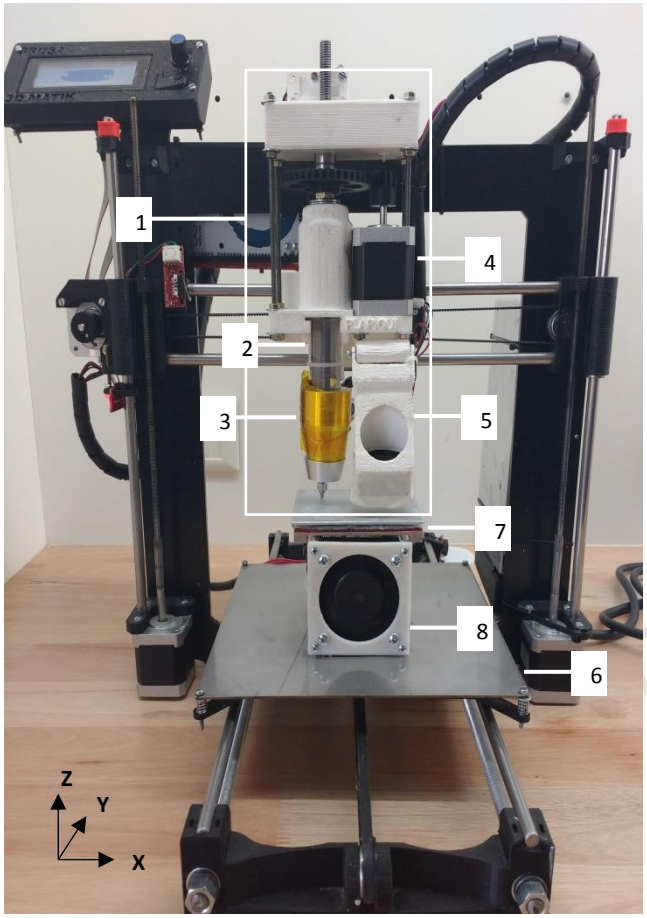

1. Printhead with X and Z-axis movement
2. Srynge
3. Heating system with temperature control
4. Plunge motion motor
5. Fan
6. Printer platform with Y-axis movement
7. Build platform
8. Peltier cooling system

Figure 1. Ad-hoc Extrusion 3D Printing system.

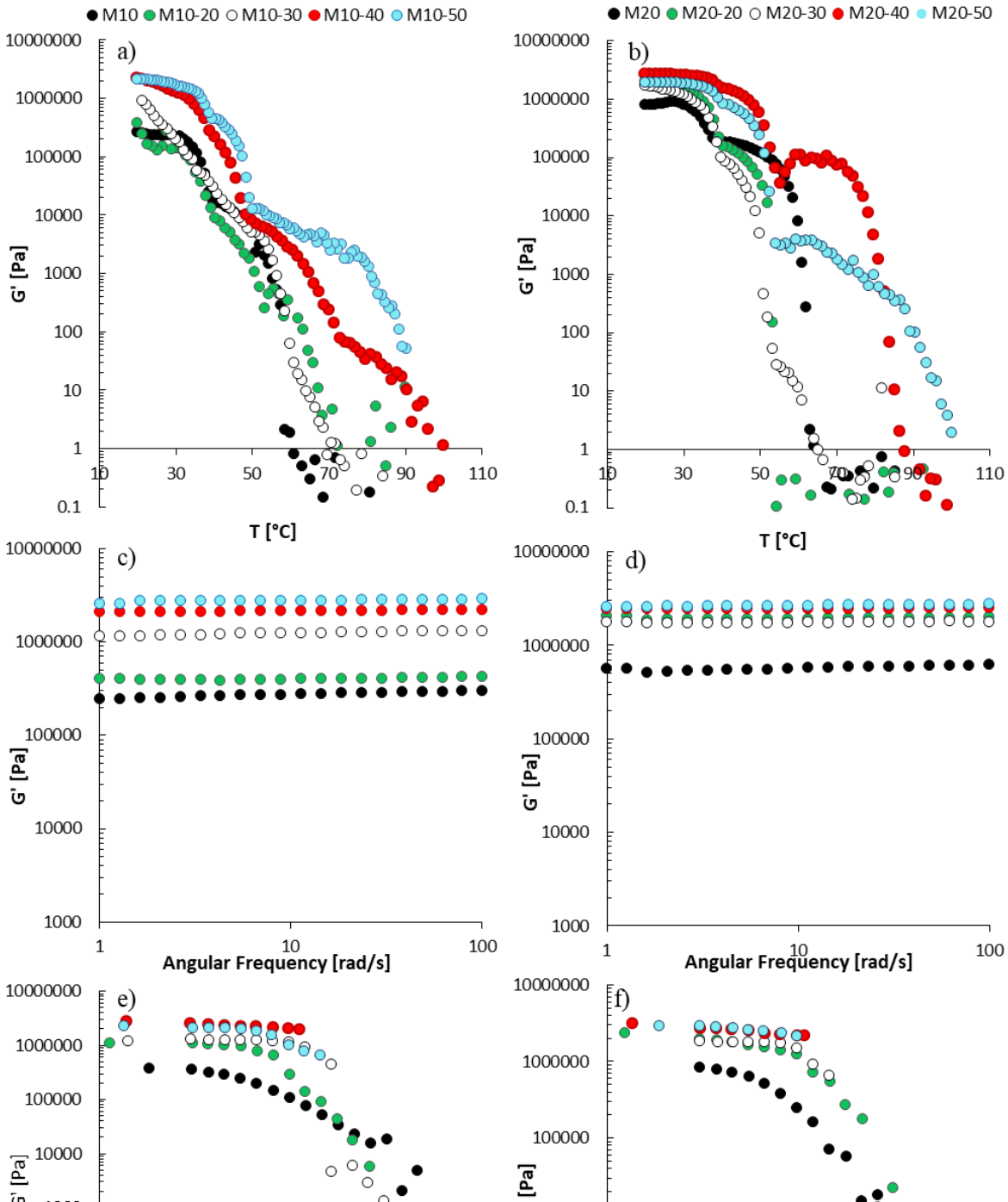
M10
M10-20
M10-30
M10-40
M10-50
a)
G' [Pa]
T [°C]
M20
M20-20
M20-30
M20-40
M20-50
b)
G' [Pa]
T [°C]
c)
G' [Pa]
Angular Frequency [rad/s]
d)
G' [Pa]
Angular Frequency [rad/s]
e)
f)

Figure 2. Rheological behavior of printing materials formulated with mixtures of 10 %wt MG (left) and 20 %wt MG (right) oleogels and variable amount of phytosterols: oscillatory temperature sweep test (top), frequency sweep test (middle), and stress sweep test (bottom). Rheological behavior of 10 and 20 %wt MG oleogels are included for comparison. All the curves represent the average behavior over at least three replicates. See nomenclature in Table 1.

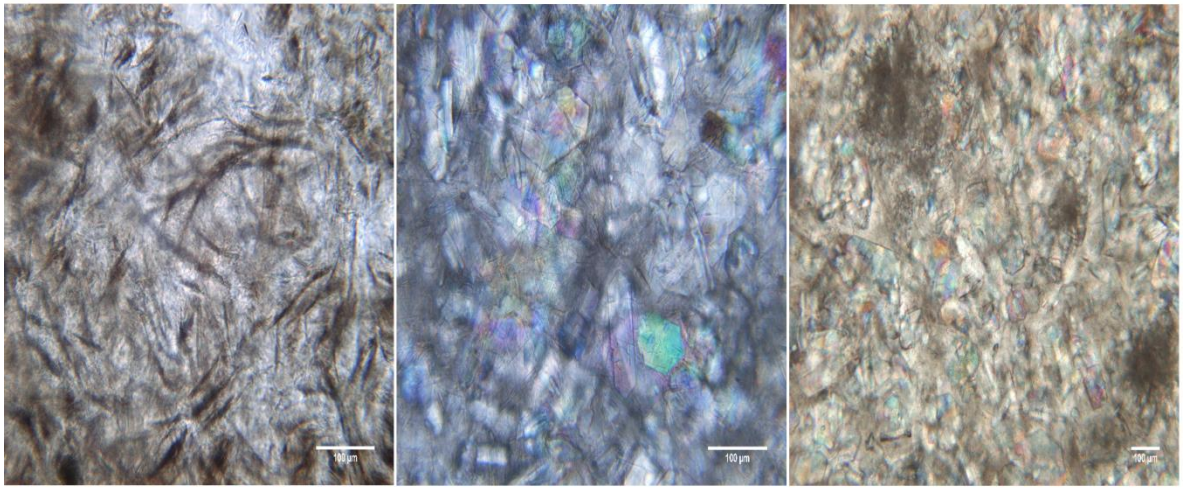

Figure 3. PLM microscopic images of the 10 %wt MG oleogel 20x (left) and a mixture of PS in HOSO 20x (middle) and 10x (right) magnification (samples temperature: 5 °C).

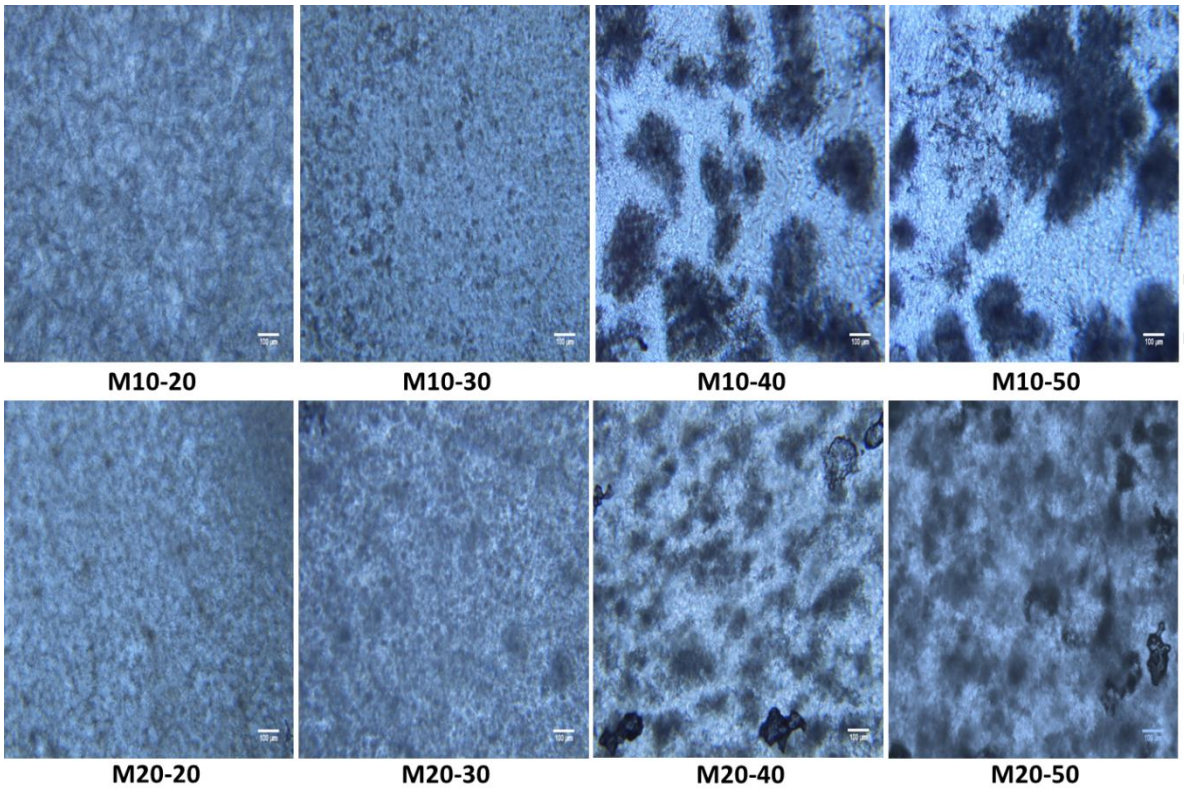

Figure 4. PLM microscopic images of mixtures containing MG oleogels and PS with 10x magnification (samples temperature: 5 °C). See nomenclature in Table 1.

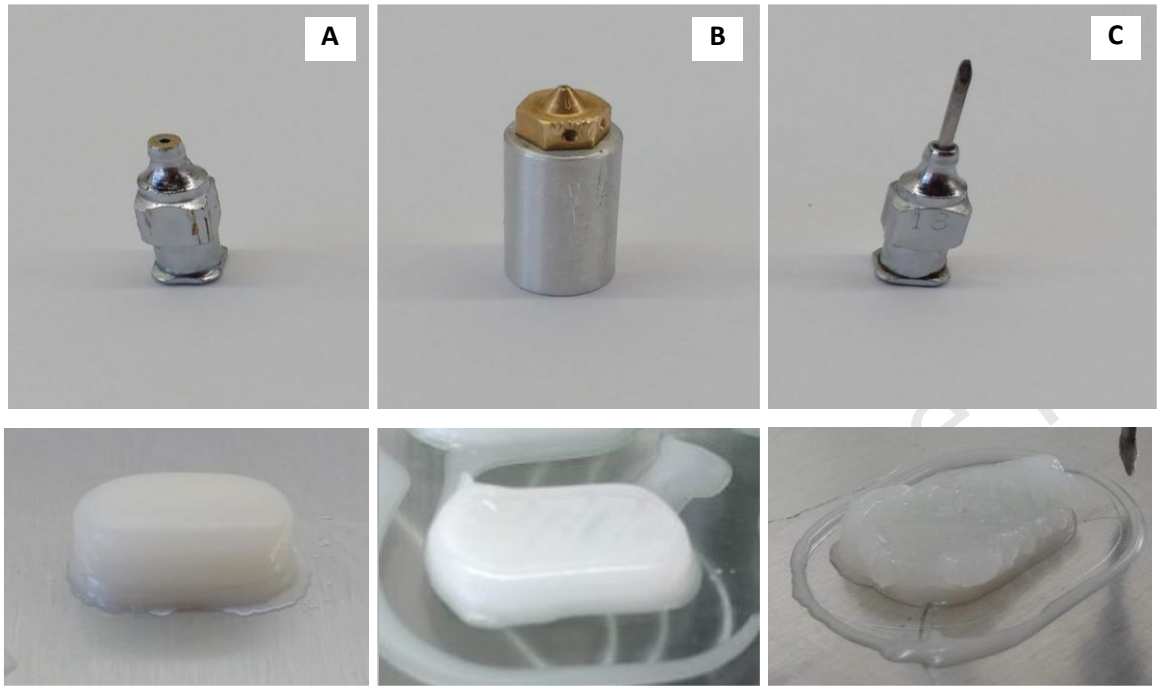

Figure 5. Types of nozzles tested for extrusion 3D printing (A, B, and C, see section 2.5 for more detail) and the corresponding solid form printed using the M10-20 (bottom).

Figure 6. Printing tests with materials formulated with 10 %wt of MG and variable amount of phytosterols.

M20-20

M20-30

M20-40

M20-50

Figure 7. Printing tests with materials formulated with 20 %wt of MG and variable amount of phytosterols.

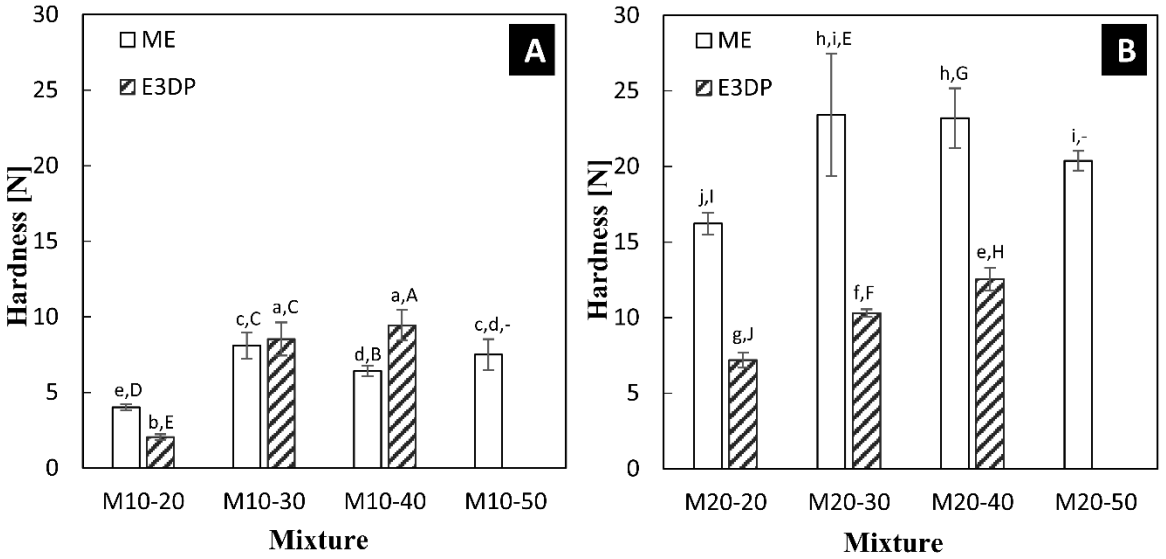

Figure 8. Hardness of oral solid forms formulated with mixtures of A) 10 %wt MG and B) 20 %wt MG oleogels and phytosterols (see nomenclature in Table 1) obtained by manual extrusion (ME) or extrusion 3D printing (E3DP). Bars represent means ± standard deviation. Significant differences between samples are represented by different letters ($p < 0.05$). The comparison between different mixtures for a specific obtention process is indicated with lowercase letters and the comparison between processes for a specific mixture is indicated with uppercase letters.

Table 1. Composition of the mixtures formulated with monoglycerides oleogels and phytosterols used as printable materials, gel point temperature (T_g), Yield stress (Y_s), and weight of printed solid forms (W).

Mixture	MG/ (HOSO+MG) (%)	PS/ (HOSO+MYV) (%)	T_g (°C)	Y_s (Pa)	W (g)	
M10*		-	59.05^{g} (0.78)	1339^{d} (65)	-	-
M10-20		20	70.43^{d} (0.62)	1738^{c} (88)	1.162	(0.008)
M10-30	10	30	73.40^{c} (1.51)	4303^{b} (253)	1.078	(0.064)
M10-40		40	86.40^{b} (0.99)	n.d	1.042	(0.028)
M10-50		50	87.30^{b} (2.71)	n.d	-	-
M20*		-	64.97^{e} (1.12)	4577^{b} (230)	-	-
M20-20		20	58.47^{f} (1.12)	5214^{a} (280)	1.216	(0.052)
M20-30	20	30	61.60^{e,f} (3.39)	5275^{a} (216)	1.144	(0.040)
M20-40		40	85.70^{b} (0.99)	n.d	1.073	(0.024)
M20-50		50	92.50^{a} (0.99)	n.d	-	-

*Properties of 10 and 20 %wt MG oleogels (M10 and M20) are included for comparison. Values in parentheses are standard deviation. Samples with the same superscripts were not significantly different ($p>0.05$)
n.d= not determined.

Table 2. Printing settings used for the production of oral dosage forms.

Mixture	T_S set (°C)	Infill (%)	Fan speed	Shell thickness (mm)	Flow (%)	Layer thickness (mm)	1° layer thickness (mm)	Printing speed (mm/s)	Infill pattern	Printability
M10-20	*110*	*47*	*off*	0.3	100	1	0.2	5	concentric lines	+++
M10-30	*110*	*40*	*off*	0.3	100	1	0.2	5	concentric lines	++
M10-40	*118*	*30*	*off*	0.3	100	1	0.2	5	concentric lines	+
M10-50	*118*	*47*	*off*	0.3	100	1	0.2	5	concentric lines	failed
M20-20	*110*	*47*	*off*	0.3	100	1	0.2	5	concentric lines	+++
M20-30	*110*	*47*	*off*	0.3	100	1	0.2	5	concentric lines	++
M20-40	*115*	*35*	*30% of printing on*	0.3	100	1	0.2	5	concentric lines	++
M20-50	*115-125*	*35*	*off*	0.3	100	1	0.2	5	concentric lines	-

Highlights

- Monoglycerides oleogels and phytosterols mixtures were used as printing materials
- An ad-hoc E3D printer with a heated syringe and a cooling build platform was used
- Correlation between formulation and printability was established
- Mixtures with gel point temperature lower than 74°C favored the building of oral forms
- Best printed forms were structurally stable, with uniform weight and shape